Promotion of TH3 (T=Si and Ge) group transfer within a tetrel bond by a cation-π interaction

Journal:	*Physical Chemistry Chemical Physics*
Manuscript ID	CP-ART-11-2021-005323.R1
Article Type:	Paper
Date Submitted by the Author:	08-Dec-2021
Complete List of Authors:	Liu, Na; Yantai University Wu, Qiaozhuo; Yantai University Li, Qingzhong; Yantai University, Scheiner, Steve; Utah State University, Department of Chemistry and Biochemistry

Journal Name

ARTICLE

Promotion of TH_3 (T=Si and Ge) group transfer within a tetrel bond by a cation-π interaction

fReceived 00th January 20xx,
Accepted 00th January 20xx

DOI: 10.1039/x0xx00000x

www.rsc.org/

Na Liu,[a] Qiaozhuo Wu,[b], Qingzhong Li[*,a], Steve Scheiner[*,b]

The possibility of the transfer of the TH_3 group across a tetrel bond is considered by ab initio calculations. The TB is constructed by pairing $PhTH_3$ (Ph=phenyl; T = Si and Ge) with bases NH_3, $NHCH_2$, and the $C_3N_2H_4$ carbene. The TH_3 moves toward the base but only by a small amount in these dimers. However, when a Be^{2+} or Mg^{2+} dication is placed above the phenyl ring, the tetrel bond strength is greatly magnified reaching up to nearly 100 kcal/mol. This dication also induces a much higher degree of transfer which can be best categorized as half-transfer for the two N-bases and a near complete transfer for the carbene.

1. Introduction

Proton transfer is an important component in numerous chemical reactions and biological systems, and has accordingly attracted a great deal of attention over the years.[1-5] Generally, proton transfer is facilitated by a strong H-bond, which is in turn dependent on both the acidity of the proton donor and the alkalinity of the acceptor, as well as substituent and cooperativity effects. Typically, electron-donating substituents on the proton acceptor and the withdrawing units on the donor enhance the strength of the H-bond.[6] There have been numerous demonstrations of H-bond cooperativity, both with other H-bonds and with other types of noncovalent interactions[7-11] which can modulate the H-bond strength as well as the proton transfer occurring within.[12-14] Recent work has demonstrated that many of these same principles, e.g. cooperativity and solvation effects,[15,16] apply to the transfer of a halogen atom when it has replaced the proton in what have come to be called halogen bonds.

The tetrel bond, TB, is an attractive interaction between the σ or π-hole on a group 14 atom, e.g. C or Si, and a base, quite similar in its foundations to both the hydrogen and halogen bonds. Because of its profound implications in various areas such as crystal materials, molecular recognition, chemical reactions, and biological systems,[17-25] this noncovalent bond has engendered a rapidly growing list of theoretical and experimental studies. Among some of the findings, the TB displays cooperativity with various sorts of other noncovalent interactions including hydrogen, halogen, chalcogen, triel, beryllium, and lithium bonds.[26-31] While our understanding of proton transfer within H-bonds is fairly thorough and that of halogen transfer is now beginning to gel, one area that has escaped scrutiny to this point surrounds the question as to what conditions might promote the transfer of a tetrel-containing group within the context of a tetrel bond.

The work described herein attacks this question for the first time. As the tetrel-containing Lewis acid, a TH_3 group is attached to a phenyl group, where T=Si and Ge. This system was chosen since aromatic compounds are ubiquitous in the fields of chemistry, materials, and biology. Aromatic units are versatile in that they can engage in various sorts of interactions such as π-π stacking,[32] cation-π,[33] and anion-π interactions.[34] Three different bases were chosen to interact with the $PhTH_3$ system. As N-bases, NH_3 and $NHCH_2$ place the N in sp^3 and sp^2 hybridizations, respectively, so can span a range of nucleophilicity. To further expand the scope of bases considered, the N-heterocyclic $C_3N_2H_4$ carbene allows the lone pair of a C atom to interact with the tetrel atom. These bases have been shown earlier to form fairly strong tetrel bonds with a small model acid SiH_3F,[35] so ought to exert a reasonable pull on the tetrel group. Very recently, such N-heterocycle carbenes have been used as electron donors to form carbon···carbon$^+$ tetrel bonds.[36] The first issue concerns how much of a tetrel group transfer occurs in any of the dimers formed by each acid when paired with each base. In order to ramp up the tendency toward a transfer, a dication Be^{2+} or Mg^{2+} is placed above the phenyl ring of the acid. This choice is guided by an earlier work wherein the tetrel bond strength of $C_6H_5TH_3\cdots NCX$ (T=Si and Ge; X=H, F and OH) was amplified by the presence of a monocation in a similar position.[37] The central question addressed is whether this cation can exert a strong enough force so as to push the TH_3 group across to the base, and if so, would this be a full or only partial transfer?

2. Theoretical methods

---

[a] The Laboratory of Theoretical and Computational Chemistry, School of Chemistry and Chemical Engineering, Yantai University, Yantai 264005, People's Republic of China. E-mail: liqingzhong1990@sina.com; Fax: +86 535 6902063; Tel: +86 535 6902063.

[b] Department of Chemistry and Biochemistry, Utah State University, Logan, UT 84322-0300, USA E-mail: steve.scheiner@usu.edu.

†Electronic Supplementary Information (ESI) available: [Figs. S1-S2 and Table S1]. See DOI: 10.1039/x0xx00000x

All calculations were performed using the Gaussian 09 program.[38] Geometries were optimized at the MP2 computational level with the aug-cc-pVTZ basis set. Frequency calculations at the same level confirmed that the structures obtained correspond to energetic minima. The interaction energy was calculated by the supermolecular method involving the energies of the monomers at the geometries they adopt within the complex. This quantity was corrected for the basis set superposition error (BSSE) by the counterpoise protocol proposed by Boys and Bernardi.[39]

Using the nature bond orbital (NBO) method[40] within the Gaussian 09 program, charge transfer and second-order perturbation energy were obtained. The AIMAll package[41] was used to assess the topological parameters at each bond critical point (BCP) including electron density, its Laplacian, and energy density. Molecular electrostatic potentials (MEPs), and their extrema, were calculated on the 0.001 a.u. isodensity surface at the MP2/cc-pVTZ level using the WFA-SAS program.[42]

3. Results

3.1 Dyads

<Figure 1>

As depicted in the top two diagrams of Figure 1, there is a σ-hole lying along the extension of the C-T bond for both T=Si and Ge. The value of V_{max} on the ρ=0.001 a.u. isodensity surface is quite similar for the two molecules between 16 and 17 kcal/mol. A nucleophile is drawn toward this σ-hole so as to form a tetrel-bonded complex. The change in hybridization of the N from sp^3 for NH_3 to sp^2 for $NHCH_2$ enhances the interaction energy even though there is little difference in the values of V_{min} in Figure S1, which are within 2% of one another. Changing the interacting atom from N to C in the $C_3N_2H_4$ carbene magnifies V_{min} to nearly -50 kcal/mol, and further strengthens the tetrel bond, albeit by only a small amount. There is also a trend for Si to engage in slightly stronger TBs than does Ge, despite their very similar V_{max}.

<Figure 2>

Figure 2a depicts a typical such TB, in this case using $C_3N_2H_4$ as the base, and illustrates the definition of the geometrical parameters. R_1 and R_2 refer respectively to the distance of the central T to the nucleophilic atom N or C, and to the C of the phenyl group, while α is equal to the average of the three C···T-H angles. Although the C-T bond elongates by a certain amount upon formation of the TB (0.009-0.018 Å), R_1 is much longer than R_2 so one cannot speak of any appreciable transfer of the TH_3 group in any of these dyads. This distinction is reflected in the R_2/R_1 ratio in Table 1, which is roughly 0.6. The $γ_1$ and $γ_2$ quantities in the last two columns of Table 1 refer each distance to the sum of vdW radii. $γ_2$ is roughly 0.5, which reflects its covalent nature, while the much larger $γ_1$ is consistent with a much weaker noncovalent bond. As a second consideration, α is close to the tetrahedral angle, so the TB has little effect on the pyramidal character of the TH_3 group.

<Table 1>

3.2 Triads

The ability of an external cation to promote a TH_3 transfer was tested by placing either of two dications, Be^{2+} or Mg^{2+} directly above the phenyl ring, as exhibited in Figure 2b. The position of the cation was optimized along with the remainder of the triad structure. One might expect that this dication would suck density out of the $PhTH_3$ unit, and thereby accentuate the σ-hole on T. This hole deepening is illustrated by the large values of V_{max} in the last four panels of Figure 1 which increases this quantity by an order of magnitude up to the 200 kcal/mol range. The magnification is somewhat larger for the more compact Be^{2+} cation.

<Figure 3>

Like the σ-hole depths, the interaction energies are also enhanced by approximately an order of magnitude by either of these two dications. E_{int}, which refers to the interaction of the base with the $M^{2+}\cdots PhTH_3$ pair, is particularly large for $C_3N_2H_4$, rising up to about 100 kcal/mol, twice that for the two N-bases, which are themselves also magnified a great deal. The α angle lies in the vicinity of 90° for these triads, indicating a relatively planar TH_3 group. In fact, α correlates rather well with the interaction energy, with a correlation coefficient of 0.94, as shown in Figure 3. A stronger TB diminishes α, getting it below 90° for the more strongly bound complexes. Such small angles are suggestive of an inversion of the TH_3 group, which is itself associated with a certain degree of transfer of TH_3 from the phenyl to the base

The R_1 and R_2 distances in Table 1 bear out this idea. R_1 is roughly equivalent to R_2 for those triads with NH_3 and $NHCH_2$, with a ratio of just slightly larger than unity. It might thus be appropriate to consider the TH_3 group as equally shared between the two subunits, a sort of half transfer. The degree of transfer is considerably larger for the carbene, where the R_2/R_1 ratio has risen to well above 1, particularly for the Be^{2+} dication, where it is 1.4. It would thus be fair to think of a TH_3 transfer that exceeds a half transfer, even approaching a full transfer. Indeed, R_1 in the $Be^{2+}\cdots PhSiH_3\cdots C_3N_2H_4$ complex is 1.960 Å, only some 0.05 Å longer than the 1.913 Å for a fully optimized $^{+}SiH_3\text{-}C_3N_2H_4$ cation monomer. The triad and monomer values in the Ge analogues are 2.023 and 1.964 Å, respectively, a difference of only 0.06 Å. Another measure of the degree of transfer arises in the α angle. A value of 90° might be thought of as a demarcation of half transfer as the TH_3 group undergoes an inversion. According to Figure 3, this line is crossed when the interaction energy exceeds about 36 kcal/mol.

<Table 2>

3.3 Degree of Transfer

Other means of assessing the degree of transfer are derived from AIM analysis of the electron density topology. The data in the first six rows of Table 2 indicate a covalent C-T bond in the six dyads, with bond critical point density > 0.1, large density Laplacian and negative energy density H. The corresponding quantities for the T···N/C bonds are clearly noncovalent: ρ and $\nabla^2ρ$ are an order of magnitude smaller, and H is slightly positive. The situation changes dramatically when the M^{2+} cations are added. All three AIM quantities are comparable for the two bonds but the balance shifts quite a bit toward a stronger and at least partially covalent T···C/N bond for the $C_3N_2H_4$ base, while the C-T bond has weakened quite a bit. Note especially that the sign of H switches from slightly positive in the dyads to substantially negative in all of the triads, clear confirmation of a strengthened covalent nature.

The NCI diagrams of the dyads and triads displayed in Figure S2 are a graphical way of looking at the electron density topology in a three-dimensional fashion. The green areas in the dyads are consistent with a weak T···N/C tetrel bond, and the covalent C-T bond to the phenyl group is signaled by the red and blue patterns. In the case of the triads, however, the patterns are similar on both sides of the TH_3 group, consistent with an interpretation of some degree of TH_3 transfer.

<Table 3>

An important feature of tetrel and other noncovalent bond formation is the transfer of charge from Lewis base to acid. This charge transfer (CT) is reported in Table 3 and is fairly small in the dyads, 0.04 e or less. This quantity is greatly magnified in the triads, comporting with their much stronger tetrel bonds. CT rises to more than 0.4 e in several cases, the triads with the highest degree of TH_3 transfer. When CT is calculated on base of Mulliken charge, its value becomes smaller, but the variation is similar to that with natural charge. In addition to an overall transfer between the two subunits, the transfer can be further partitioned into pairs of orbitals. As is common to tetrel and related bonds, the largest transfer is that from the lone pair of the C/N atom of the Lewis base into the $\sigma^*_{(C\text{-}T)}$ antibonding orbital of the acid. The overlap between these orbitals is illustrated in Figure 4a. As seen in the fourth column of Table 3, the second-order perturbation energy associated with this transfer E^2 is between 5 and 10 kcal/mol for the various dyads. As the tetrel bond is strengthened in the triads, and the TH_3 group moves closer to the base, this quantity is drastically enhanced, reaching the 88-400 kcal/mol range. Note also that due to the half transfer, there is a mirror image tetrel bond between the T and the phenyl group, exemplified by Figure 4b. The NBO charge transfer energies for this second TB are listed in the last column of Table 3. In the Be^{2+} cases, this second quantity is smaller than the first, consistent with a transfer of the TH_3 to the base. This same disparity occurs in the Mg^{2+} cases with the carbene base; NBO suggests the bond to the phenyl group remains stronger than that to the base for NH_3 and $NHCH_2$.

<Figure 4>

With specific regard to the motion of the central TH_3 between the phenyl and base, this issue can be alternately viewed by considering the energy of the system with respect to both R_2 and its sum with R_1. Figure 5 plots the total energy of the system as cuts through this two-dimensional surface for the $PhSiH_3 \cdots C_3N_2H_4$ dyad in 5a and the same system but with Be^{2+} added in 5b. Each colored curve was computed by fixing the intermolecular distance between the acid and base $R(C\cdots C)=R_1+R_2$ to a particular value. Then a SiH_3 transfer potential was computed by altering the C-Si bond length within the $PhSiH_3$ unit, holding the intermolecular distance fixed. In the $PhSiH_3 \cdots C_3N_2H_4$ dyad, all curves of Figure 5a contain a single well with a relatively short R(C-Si), thus signaling no transfer. But after the Be^{2+} has been added, each curve in Figure 5b contains two wells, suggesting a transfer is possible at any particular frozen intermolecular distance. The two wells are of different energy, with the untransferred $PhSiH_3 \cdots C_3N_2H_4$ more stable than $Ph \cdots SiH_3C_3N_2H_4$. They are separated by an energy barrier of variable height. For example, with $R(C\cdots C)$ fixed at 4.6 Å, an energy barrier of 9.4 kcal/mol separates the two minima. The barrier is sensitive to the intermolecular distance, increasing quickly as $R(C\cdots C)$ is elongated, with some of these values contained in Table S1.

<Figure 5>

4. Discussion

It would thus appear that the degree of transfer of the TH_3 group from the phenyl ring to any of several bases is rather small for both Si and Ge in the dimers. The C-T distance stretches by less than 0.02 Å, and in some cases less than 0.01 Å. This minimal transfer is understandable since a full transfer would lead to an ion pair involving $C_6H_5^-$ and $^+TH_3$-Nuc. This reluctance for an overall neutral complex to engage in more than a small amount of transfer places the TH_3 group in the same category as the closely related proton transfer in H-bonded systems, according to an extensive body of literature that has accumulated over the years.[43-45] And more recent examination of the closely related halogen transfer[46-49] has arrived at a similar conclusion as the tetrel transfer here.

Again for both H-bonds and halogen bonds, the situation changes when the entire system contains either an overall positive or negative charge. In such a case, the transfer no longer transitions the system from a neutral to a much less stable ion pair. Instead, the $(AH^+ \cdots B) \rightarrow (A \cdots H^+B)$ reaction simply changes an ion-neutral complex to a very similar neutral-ion dimer, with no obvious or dramatic change in energy. Work over the years has shown that systems of this type, whether H- or halogen-bonded, are characterized by a double-well potential, with an energy barrier that rises quickly as the distance between the A and B subunits is stretched. [50-56]

The calculations described above show how the presence of a cation can act to push a TH_3 group across a tetrel bond. This finding conforms to earlier work, for example in that a proton transfer can be promoted by the presence of an ion[57-60] as can the presence of neighboring dipoles.[61] There are environments which might enable the transfer within a neutral system. Solvation for example, helps to stabilize the ion pair thus facilitating the proton transfer within a neutral complex[62] and can perturb the potential within a charged system as well.[55] There are also cooperative effects that can push an ionic entity across an existing noncovalent bond[63] as did the dications here.

It is worth mentioning that the half transfer of any of these TH_3 groups would correspond approximately to the transition state in a S_N2 reaction. In contrast, though, these complexes where α is roughly 90° correspond to minima, not a transition state. The S_N2 reaction is usually discussed in the context of T=C, but the systems contained here did not contain the methyl group, i.e. T was not set equal to C. In the S_N2 reaction involving the CH_3 group, an anion is often taken as nucleophile, wherein the CH_3 group transfers from a weak nucleophile to a strong one. When $PhCH_3$ pairs with NH_3, $NHCH_2$, and $C_3N_2H_4$, the interaction is very weak, less than 1 kcal/mol. However, no TB is obtained even when a dication is added. In future work, we intend to focus on the CH_3 transfer through the intermediacy of a tetrel bond.

5. Conclusions

The transfer of a TH_3 group (T=Si and Ge) can be realized, even though this group is much heavier than a proton and is in principle much more difficult to accomplish. The ease of this transfer is closely related to the strength of the tetrel bond within the complex. Even when paired with any of three strong bases, NH_3, $NHCH_2$, and the carbene $C_3N_2H_4$, the TH_3 group of $PhTH_3$ will not transfer, due in part to its shallow σ-hole. On the other hand, introduction of a Be^{2+} or Mg^{2+} dication above the phenyl ring deepens the σ-hole, and greatly strengthens the tetrel bond, up to the 100 kcal/mol range. In such a situation, the TH_3 group transfers roughly halfway for the two N-bases, and more completely for the carbine.

Acknowledgements

This work was supported by the Natural Science Foundation of Shandong Province (ZR2021MB123), the US National Science Foundation (1954310), and the Yantai University Innovation Foundation (YDZD2111).

References

1 H. C. Xi, Z. P. Zhang, W. W. Zhang, M. Q. Li, C. Lian, Q. F. Luo, H. Tian, W. H. Zhu, *J. Am. Chem. Soc.* 2019, **141**, 18467-18474.

2 H. Tai, S. Hirota, S. T. Stripp, *Acc. Chem. Res.* 2021, **54**, 232-241.

3 G. Cassone, *J. Phys. Chem. Lett*. 2020, **11**, 8983-8988.

4 Z. Y. Liu, J. W. Hu, T. H. Huang, K. Y. Chen, P. T. Chou, *Phys. Chem. Chem. Phys*. 2020, **22**, 22271-22278.

5 Y. Sugo, K. Saito, H. Ishikita, *Proc. Natl. Acad. Sci. USA.* 2021, **118**, e2103203118.

6 J. Reynisson, E. McDonald, *J. Comput. Aid. Mol. Des*. 2004, **18**, 421-431.

7 J. M. Guevara-Vela, E. Romero-Montalvo, V. A. M. Gómez, R. Chávez-Calvillo, M. García-Revilla, E. Francisco, T. Rocha-Rinza, *Phys. Chem. Chem. Phys*. 2016, **18**, 19557-19566.

8 T. Kar, S. Scheiner, *J. Phys. Chem. A* 2004, **108**, 9161-9168.

9 Q. Z. Li, Q. Q. Lin, W. Z. Li, J. B. Cheng, B. A. Gong, J. Z. Sun, *ChemPhysChem* 2018, **9**, 2265-2269.

10 N. Dominelli-Whiteley, J. J. Brown, K. B. Muchowska, I. K. Mati, C. Adam, T. A. Hubbard, S. L. Cockroft, *Angew. Chem. Int. Ed*. 2017, **129**, 7766-7770.

11 O. Mo, M. Yanez, I. Alkorta, J. Elguero, *J. Chem. Theory. Comput.* 2012, **8**, 2293-2300.

12 O. Mo, M. Yáñez, J. E. Del Bene, I. Alkorta, J. Elguero, *ChemPhysChem* 2005, ***6***, 1411-1418.

13 O. Mó, M. Yáñez, I. Alkorta, J. Elguero, *Mol. Phys*. 2014, **112**, 592-600.

14 Q. Yu, X. D. Zhang, S. T. Wu, H. Y. Chen, Q. L. Zhang, H. Xu, Y. L. Huang, B. X. Zhu, X. L. Ni, *Chem. Commun*. 2020, **56**, 2304-2307.

15 H. L. Xu, Q. Z. Li, S. Scheiner, *ChemPhysChem* 2018, **19**, 1456-1464.

16 P. Calvo, J. Crugeiras, A. Rios, *J. Org. Chem.* 2009, **74**, 5381-5389.

17 A. Bauzá, J. Tiddo, T. J. Mooibroek, A. Frontera, *Angew. Chem. Int. Ed.* 2013, **125**, 12543-12547.

18 S. J. Grabowski, *Phys. Chem. Chem. Phys.* 2014, **16**, 1824-1834.

19 A. Bauzá, T. J. Mooibroek, A. Frontera, *Chem. Commun*. 2014, **50**, 12626-12629.

20 J. E. Del Bene, I. Alkorta, J. Elguero, *J. Phys. Chem. A* 2017, **121**, 4039-4047.

21 S. Scheiner, *J. Phys. Chem. A* 2017, **121**, 3606-3615.

22 A. Robertazzi, J. A. Platts, P. Gamez, *ChemPhysChem* 2014, **15**, 912-917.

23 A. Frontera, R. Ramis, A. Bauzá, *Comput. Theor. Chem*. 2014, **1038**, 67-70.

24 G. Mahmoudi, A. Bauzá, A. Frontera, *Dalton Trans.* 2016, **45**, 4965-4969.

25 Q. Z. Li, X. Guo, X. Yang, W. Z. Li, J. B. Cheng, H. B. Li, *Phys. Chem. Chem. Phys.* 2014, **16**, 11617-11625.

26 M. Marín-Luna, I. Alkorta, J. Elguero, *J. Phys. Chem. A* 2016, **120**, 648-656.

27 I. Alkorta, M. M. Montero-Campillo, O. Mó, J. Elguero, M. Yáñez, *J. Phys. Chem. A* 2019, **123**, 7124-7132.

28 M. X. Liu, L. Yang, Q. Z. Li, W. Z. Li, J. B. Cheng, *J. Mol. Model.* 2016, **22**, 1-10.

29 X. Guo, Y. W. Liu, Q. Z. Li, W. Z. Li, J. B. Cheng, *Chem. Phys. Lett*. 2015, **620**, 7-12.

30 M. Solimannejad, M. Orojloo, S. Amani. *J. Mol. Model.* 2015, **21**, 183.

31 Q. Tang, Q. Z. Li, *Comput. Theor. Chem*. 2014, **1050**, 51-57.

32 T. Caronna, R. Liantonio, T. A. Logothetis, P. Metrangolo, T. Pilati, G. Resnati, *J. Am. Chem. Soc*. 2004, **126**, 4500-4501.

33 J. C. Ma, D. A. Dougherty, *Chem. Rev*. 1997, **97**, 1303-1324.

34 B. L. Schottel, H. T. Chifotides, K. R. Dunbar, *Chem. Soc. Rev.* 2008, **37**, 68-83.

35 M. X. Liu, Q. Z. Li, W. Z. Li, J. B. Cheng, *Struct. Chem*. 2017, **28**, 823-831.

36 M. de las Nieves-Piña, A. Frontera, T. J. Mooibroek, A. Bauzá, *ChemPhysChem* 2021, **22**, 2478-2483.

37 M. D. Esrafili, F. Mohammadian-Sabet, *Mol. Phys*. 2016, **114**, 83-91.

38 M. J. Frisch, G. W. Trucks, H. B. Schlegel, G. E. Scuseria, A. Robb, J. R. Cheeseman, G. Scalmani, V. Barone, B. Mennucci, G. A. Petersson, H. Nakatsuji, M. Caricato, X. Li,H. P. Hratchian, A. F. Izmaylov, J. Bloino, G. Zheng,J. L. Sonnenberg, M. Hada, M. Ehara, K. Toyota, R. Fukuda,J. Hasegawa, M. Ishida, T. Nakajima, Y. Honda, O. Kitao,H. Nakai, T. Vreven, J. Montgomery, J. E. Peralta, F. Ogliaro, M. Bearpark, J.J. Heyd, E. Brothers, K. N.Kudin,V. N. Staroverov, R. Kobayashi, J. Normand, K. Raghavachari,A. Rendell, J. C. Burant, S. S. Iyengar, J. Tomasi, M. Cossi, N. Rega, J. M. Millam, M. Klene, J. E. Knox, J. B. Cross,V. Bakken, C. Adamo,J. Jaramillo, R. Gomperts,R.E. Stratmann,O. Yazyev, A. J. Austin, R.

Cammi,C. Pomelli, J. W. Ochterski, R. L. Martin, K. Morokuma, V. G. Zakrzewski, G. A. Voth, P. Salvador, J. J. Dannenberg,S. Dapprich, A. D. Daniels, O. Farkas, J. B. Foresman, J. V. Ortiz, J. Cioslowski, D. J. Fox, Gaussian 09, RevisionD.01, Inc, Wallingford, CT 2009.

39 S. F. Boys, F. Bernardi, *Mol. Phys*. 1970, **19**, 553-566.

40 A. E. Reed, L. A. Curtiss, F. Weinhold, *Chem. Rev*. 1988, 88, 899-926.

41 T. A. Keith, AIMALL, version 13.05.06, TK Gristmill Software: Overland Park, KS, 2013.

42 F. A. Bulat, A. Toro-Labbé, T. Brinck, J. S. Murray, P. Politzer, *J. Mol. Model*. 2010, **16**, 1679-1691.

43 A. C. Legon, A. L. Wallwork, C. A. Rego, *J. Chem. Phys*. 1990, **92**, 6397-6407.

44 L. Vanderheyden, G. Maes, T. Zeegers-Huyskens, *J. Mol. Struct*. 1984, **114**, 165-172.

45 L. Schriver, A. Schriver, J. P. Perchard, *J. Am. Chem. Soc.* 1983, **105**, 3843-3848.

46 J. E. Del Bene, I. Alkorta, J. Elguero, *J. Phys. Chem. A* 2014, **118**, 2360-2366.

47 I. Alkorta, J. Elguero, *ChemPhysChem* 2016, **17**, 3112-3119.

48 S. M. Chalanchi, I. Alkorta, J. Elguero, D. Quiñonero, *ChemPhysChem.* 2017, **18**, 3462-3468.

49 J. Lu, S. Scheiner, *Comput. Theor. Chem.* 2021, **1204**, 113398.

50 J. Lu, S. Scheiner, *Chem. Phys. Lett.* 2019, **731**, 136593.

51 S. Scheiner, L. Wang, *J. Am. Chem. Soc.* 1993, **115**, 1958-1963.

52 S. Scheiner, E. A. Hillenbrand, *Proc. Nat. Acad. Sci. U. S. A.* 1985, **82**, 2741-2745.

53 S. Scheiner, *Acc. Chem. Res.* 1985, 18, 174-180.

54 E. A. Hillenbrand, S. Scheiner, *J. Am. Chem. Soc.* 1984, **106**, 6266-6273.

55 S. Scheiner, X. Duan, *Phys. Chem. Chem. Phys.* 1991, **60**, 874-883.

56 S. Scheiner, *J. Chem. Phys*. 1982, **77**, 4039-4050.

57 S. Scheiner, P. Redfern, M. M. Szczesniak, *J. Phys. Chem.* 1985, **89**, 262-266.

58 M. M. Szczesniak, S. Scheiner, *J. Phys. Chem.* 1985, **89**, 1835-1840.

59 I. J. Kurnig, S. Scheiner, *Int. J. Quantum Chem.* 1986, **13**, 71-79.

60 S. Scheiner, T. Das, *Int. J. Quantum Chem*. 1988, **34**, 137-147.

61 S. Scheiner, R. Wang, L. Wang, *Int. J. Quantum Chem.* 1989, **36**, 211-217.

62 I. J. Kurnig, S. Scheiner, *Int. J. Quantum Chem*. 1987, **14**, 47-56.

1. M. C. Hou, Q. Z. Li, S. Scheiner, *Chem. Phys. Lett.* 2019, **731**, 136584.

Journal Name

ARTICLE

Table 1. Interaction energy of tetrel bond (E_{int}, kcal/mol), average of three C···T-H angles (α, deg), intermolecular separation (R_1, Å), C-T bond length (R_2, Å) and its change (ΔR_2, Å) in the dyads and triads

Complex	E_{int}	α	R_1	R_2	ΔR_2	R_2/R_1	γ_1	γ_2
$PhSiH_3\cdots NH_3$	-1.94	108.1	3.112	1.886	0.009	0.61	0.853	0.496
$PhSiH_3\cdots NHCH_2$	-2.52	107.9	3.050	1.887	0.010	0.62	0.836	0.497
$PhSiH_3\cdots C_3N_2H_4$	-3.90	106.1	2.942	1.895	0.018	0.64	0.770	0.499
$PhGeH_3\cdots NH_3$	-1.76	108.1	3.222	1.940	0.009	0.60	0.882	0.510
$PhGeH_3\cdots NHCH_2$	-2.22	107.9	3.123	1.940	0.009	0.62	0.856	0.510
$PhGeH_3\cdots C_3N_2H_4$	-3.19	107.3	3.092	1.945	0.014	0.63	0.814	0.512
$Be^{2+}\cdots PhSiH_3\cdots NH_3$	-40.82	89.1	2.072	2.155	0.268	1.04	0.545	0.567
$Be^{2+}\cdots PhSiH_3\cdots NHCH_2$	-44.56	88.8	2.031	2.161	0.274	1.06	0.534	0.569
$Be^{2+}\cdots PhSiH_3\cdots C_3N_2H_4$	-100.06	78.9	1.960	2.689	0.802	1.37	0.516	0.708
$Be^{2+}\cdots PhGeH_3\cdots NH_3$	-34.71	89.7	2.182	2.276	0.345	1.04	0.574	0.599
$Be^{2+}\cdots PhGeH_3\cdots NHCH_2$	-37.60	89.1	2.141	2.281	0.350	1.07	0.563	0.600
$Be^{2+}\cdots PhGeH_3\cdots C_3N_2H_4$	-94.49	76.3	2.023	2.850	0.919	1.41	0.532	0.750
$Mg^{2+}\cdots PhSiH_3\cdots NH_3$	-20.88	91.5	2.123	2.084	0.197	0.98	0.558	0.548
$Mg^{2+}\cdots PhSiH_3\cdots NHCH_2$	-30.01	91.2	2.078	2.087	0.200	1.00	0.547	0.549
$Mg^{2+}\cdots PhSiH_3\cdots C_3N_2H_4$	-66.10	86.5	2.018	2.220	0.333	1.10	0.531	0.584
$Mg^{2+}\cdots PhGeH_3\cdots NH_3$	-24.14	93.0	2.260	2.174	0.243	0.96	0.598	0.572
$Mg^{2+}\cdots PhGeH_3\cdots NHCH_2$	-27.34	92.5	2.215	2.176	0.245	0.98	0.583	0.573
$Mg^{2+}\cdots PhGeH_3\cdots C_3N_2H_4$	-69.56	83.0	2.072	2.504	0.573	1.21	0.545	0.715

Note: γ is a ratio of R_1 or R_2 to the sum of the van der Waals radii of the two atoms.

Table 2. Electron density (ρ), Laplacian ($\nabla^2\rho$), and total energy density (*H*) at the C-T and T···N/C BCPs in the dyads and triads, all in a.u.

Complex	C-T			T···N/C		
	ρ	$\nabla^2\rho$	*H*	ρ	$\nabla^2\rho$	*H*
$PhSiH_3\cdots NH_3$	0.1084	0.3729	-0.0466	0.0091	0.0284	0.0008
$PhSiH_3\cdots NHCH_2$	0.1084	0.3734	-0.0466	0.0104	0.0319	0.0009
$PhSiH_3\cdots C_3N_2H_4$	0.1073	0.3679	-0.0459	0.0133	0.0335	0.0007
$PhGeH_3\cdots NH_3$	0.1260	0.1507	-0.0713	0.0082	0.0258	0.0009
$PhGeH_3\cdots NHCH_2$	0.1259	0.1521	-0.0712	0.0104	0.0307	0.0009
$PhGeH_3\cdots C_3N_2H_4$	0.1242	0.1540	-0.0696	0.0120	0.0333	0.0008
$Be^{2+}\cdots PhSiH_3\cdots NH_3$	0.0586	0.1775	-0.0184	0.0590	0.2180	-0.0130
$Be^{2+}\cdots PhSiH_3\cdots NHCH_2$	0.0577	0.1743	-0.0180	0.0600	0.2537	-0.0126
$Be^{2+}\cdots PhSiH_3\cdots C_3N_2H_4$	0.0232	0.0395	-0.0033	0.0892	0.3547	-0.0294
$Be^{2+}\cdots PhGeH_3\cdots NH_3$	0.0602	0.1279	-0.0191	0.0618	0.1814	-0.0167
$Be^{2+}\cdots PhGeH_3\cdots NHCH_2$	0.0594	0.1278	-0.0186	0.0661	0.2057	-0.0184
$Be^{2+}\cdots PhGeH_3\cdots C_3N_2H_4$	0.0192	0.0497	0.0001	0.1053	0.2152	-0.0503
$Mg^{2+}\cdots PhSiH_3\cdots NH_3$	0.0695	0.2294	-0.0227	0.0510	0.1746	-0.0128
$Mg^{2+}\cdots PhSiH_3\cdots NHCH_2$	0.0690	0.2287	-0.0225	0.0544	0.2069	-0.0125
$Mg^{2+}\cdots PhSiH_3\cdots C_3N_2H_4$	0.0527	0.1312	-0.0174	0.0786	0.3006	-0.0997
$Mg^{2+}\cdots PhGeH_3\cdots NH_3$	0.0766	0.1482	-0.0305	0.0522	0.1504	-0.0118
$Mg^{2+}\cdots PhGeH_3\cdots NHCH_2$	0.0763	0.1490	-0.0303	0.0562	0.1692	-0.0135
$Mg^{2+}\cdots PhGeH_3\cdots C_3N_2H_4$	0.0396	0.0743	-0.0070	0.0938	0.1531	-0.0444

Table 3. Charge transfer of tetrel bond (CT, e) based on natural charge (N) and Mulliken charge (M) and second-order perturbation energies (E^2, kcal/mol) in the dyads and triads

complexes	CT_N	CT_M	types	E^2	types	E^2
$PhSiH_3 \cdots NH_3$	0.019	0.016	$Lp_N \rightarrow \sigma^*_{C\text{-}Si}$	5.22		
$PhSiH_3 \cdots NHCH_2$	0.019	0.018	$Lp_N \rightarrow \sigma^*_{C\text{-}Si}$	5.35		
$PhSiH_3 \cdots C_3N_2H_4$	0.041	0.035	$Lp_C \rightarrow \sigma^*_{C\text{-}Si}$	10.66		
$PhGeH_3 \cdots NH_3$	0.016	0.011	$Lp_N \rightarrow \sigma^*_{C\text{-}Ge}$	4.99		
$PhGeH_3 \cdots NHCH_2$	0.018	0.015	$Lp_N \rightarrow \sigma^*_{C\text{-}Ge}$	5.13		
$PhGeH_3 \cdots C_3N_2H_4$	0.037	0.026	$Lp_C \rightarrow \sigma^*_{C\text{-}Ge}$	10.37		
$Be^{2+} \cdots PhSiH_3 \cdots NH_3$	0.224	0.089	$Lp_N \rightarrow p^*_{Si}$	143.11	$Lp_C \rightarrow \sigma^*_{Si\text{-}N}$	31.34
$Be^{2+} \cdots PhSiH_3 \cdots NHCH_2$	0.235	0.094	$Lp_N \rightarrow p^*_{Si}$	162.27	$Lp_C \rightarrow \sigma^*_{Si\text{-}N}$	32.98
$Be^{2+} \cdots PhSiH_3 \cdots C_3N_2H_4$	0.422	0.297	$Lp_C \rightarrow p^*_{Si}$	400.69	$Lp_C \rightarrow \sigma^*_{Si\text{-}C}$	24.64
$Be^{2+} \cdots PhGeH_3 \cdots NH_3$	0.203	0.073	$Lp_N \rightarrow p^*_{Ge}$	192.53	$Lp_C \rightarrow \sigma^*_{Ge\text{-}N}$	28.76
$Be^{2+} \cdots PhGeH_3 \cdots NHCH_2$	0.205	0.082	$Lp_N \rightarrow p^*_{Ge}$	127.31	$Lp_C \rightarrow \sigma^*_{Ge\text{-}N}$	28.32
$Be^{2+} \cdots PhGeH_3 \cdots C_3N_2H_4$	0.426	0.350	$Lp_C \rightarrow p^*_{Ge}$	382.97	$Lp_C \rightarrow \sigma^*_{Ge\text{-}C}$	21.93
$Mg^{2+} \cdots PhSiH_3 \cdots NH_3$	0.205	0.055	$Lp_N \rightarrow p^*_{Si}$	117.34	$Lp_C \rightarrow p^*_{Si}$	235.74
$Mg^{2+} \cdots PhSiH_3 \cdots NHCH_2$	0.215	0.061	$Lp_N \rightarrow p^*_{Si}$	134.56	$Lp_C \rightarrow p^*_{Si}$	224.88
$Mg^{2+} \cdots PhSiH_3 \cdots C_3N_2H_4$	0.388	0.235	$Lp_C \rightarrow p^*_{Si}$	307.92	$Lp_C \rightarrow \sigma^*_{Si\text{-}C}$	29.57
$Mg^{2+} \cdots PhGeH_3 \cdots NH_3$	0.164	0.024	$Lp_N \rightarrow p^*_{Ge}$	88.39	$Lp_C \rightarrow p^*_{Ge}$	222.85
$Mg^{2+} \cdots PhGeH_3 \cdots NHCH_2$	0.172	0.041	$Lp_N \rightarrow p^*_{Ge}$	104.90	$Lp_C \rightarrow p^*_{Ge}$	209.10
$Mg^{2+} \cdots PhGeH_3 \cdots C_3N_2H_4$	0.321	0.191	$Lp_C \rightarrow p^*_{Ge}$	203.17	$Lp_C \rightarrow \sigma^*_{Ge\text{-}C}$	19.43

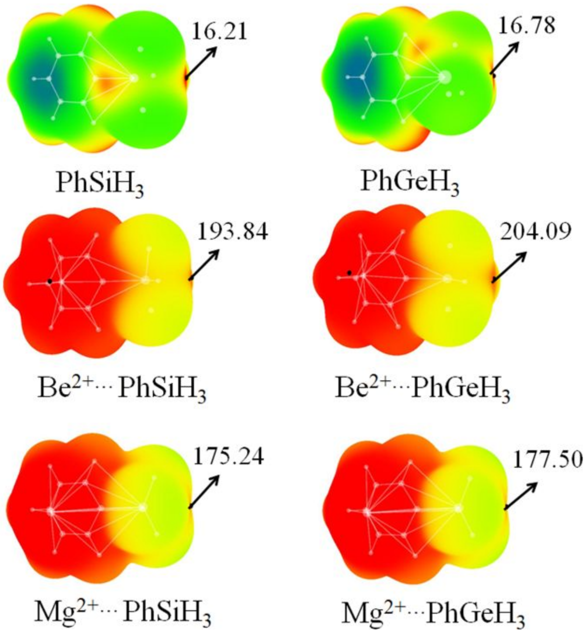

Fig. 1. MEP maps of monomers and complexes. Color ranges are: red, greater than 12; yellow, between 12 and zero; green, between zero and -12; blue, less than -12; all in kcal/mol

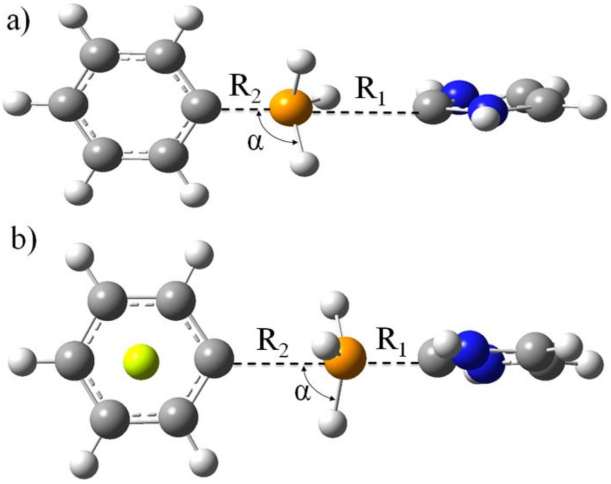

Fig. 2 The geometries of a) PhTH$_3$···C$_3$N$_2$H$_4$ and b) M^{2+}···PhTH$_3$···C$_3$N$_2$H$_4$

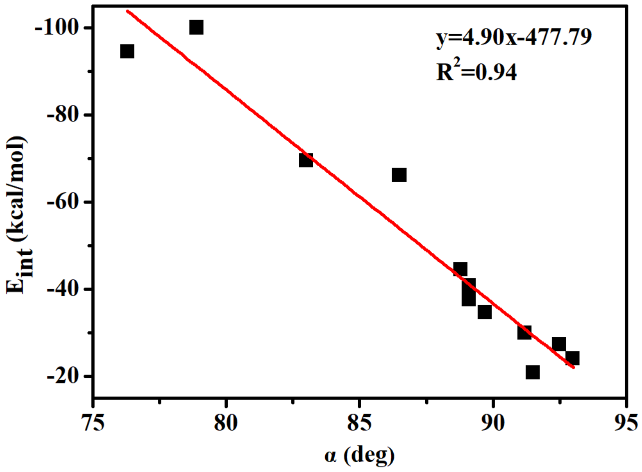

Fig. 3 Average of three C···T-H angles (α) versus the interaction energy (E_{int}) of tetrel bond in the triads.

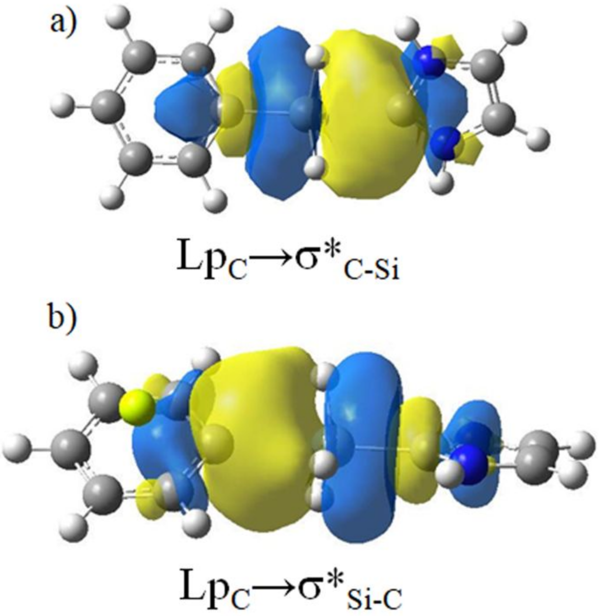

Fig. 4 Diagrams of orbital interactions in a) $PhSiH_3 \cdots C_3N_2H_4$ and b) $Be^{2+} \cdots PhSiH_3 \cdots C_3N_2H_4$.

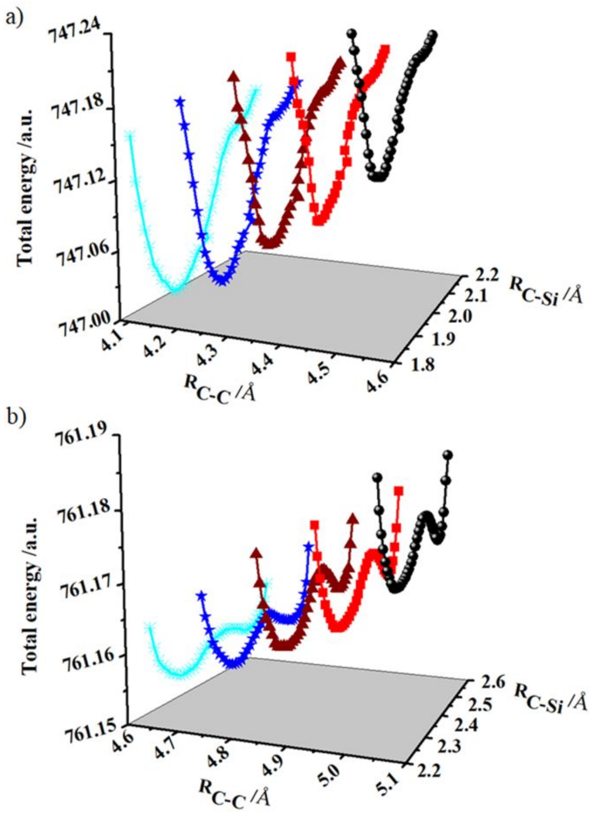

Fig. 5 Energy profiles for SiH$_3$ transfer between two carbon atoms in a) PhSiH$_3$···C$_3$N$_2$H$_4$ and b) Be^{2+}···PhSiH$_3$···C$_3$N$_2$H$_4$.